AIP | Applied Physics Letters

Tailored probes for atomic force microscopy fabricated by two-photon polymerization

Gerald Göring, Philipp-Immanuel Dietrich, Matthias Blaicher, Swati Sharma, Jan G. Korvink, Thomas Schimmel, Christian Koos, and Hendrik Hölscher

Citation: Applied Physics Letters **109**, 063101 (2016); doi: 10.1063/1.4960386
View online: http://dx.doi.org/10.1063/1.4960386
View Table of Contents: http://scitation.aip.org/content/aip/journal/apl/109/6?ver=pdfcov
Published by the AIP Publishing

Tailored probes for atomic force microscopy fabricated by two-photon polymerization

Gerald Göring,[1,a] Philipp-Immanuel Dietrich,[2,3,a] Matthias Blaicher,[2,3] Swati Sharma,[2] Jan G. Korvink,[2] Thomas Schimmel,[1,4] Christian Koos,[2,3] and Hendrik Hölscher[2,b]
[1]Institute of Nanotechnology (INT), Karlsruhe Institute of Technology (KIT), Hermann-von-Helmholtz-Platz 1, 76344 Eggenstein-Leopoldshafen, Germany
[2]Institute for Microstructure Technology (IMT), Karlsruhe Institute of Technology (KIT), Hermann-von-Helmholtz-Platz 1, 76344 Eggenstein-Leopoldshafen, Germany
[3]Institute of Photonics and Quantum Electronics (IPQ), Karlsruhe Institute of Technology (KIT), Engesserstraße 5, 76131 Karlsruhe, Germany
[4]Institute of Applied Physics (APH), Karlsruhe Institute of Technology (KIT), Wolfgang-Gaede-Straße 1, 76131 Karlsruhe, Germany

(Received 30 May 2016; accepted 16 June 2016; published online 8 August 2016)

3D direct laser writing based on two-photon polymerization is considered as a tool to fabricate tailored probes for atomic force microscopy. Tips with radii of 25 nm and arbitrary shape are attached to conventionally shaped micro-machined cantilevers. Long-term scanning measurements reveal low wear rates and demonstrate the reliability of such tips. Furthermore, we show that the resonance spectrum of the probe can be tuned for multi-frequency applications by adding rebar structures to the cantilever. *Published by AIP Publishing.* [http://dx.doi.org/10.1063/1.4960386]

The performance of scanning-probe microscopy systems significantly depends on the shape, size, and composition of the probing tip.[1,2] In practically all cases, the tip radius should be as small as possible to obtain a high lateral resolution. The overall shape of the tip, however, is frequently also important.[3] The width and height of the tip, for example, are essential features that limit the imaging of deep trenches, and specific applications require even more advanced tip designs, e.g., to image surface structures on sidewalls[4] or 3D freeform structures.

Moreover, for the case of atomic-force microscopy (AFM), not only the tip but also the cantilever is a significant component governing the behaviour of the probe. Different spring constants of the cantilever are typically used depending on whether the system is operated in contact (<1 N/m) or dynamic mode AFM (>1 N/m). Furthermore, several designs extending the simple rectangular cantilever shape have been developed in order to allow for the analysis of tip-sample interactions during imaging.[5–7] Commercial AFM cantilevers are commonly rectangular or V-shaped and are micro-machined from silicon and silicon nitride.[1,2] Both types are commercially available with a large variety of geometries and with different types of tips. Typically, these tips are micro-machined during the production of the probe.[8] Due to the limitations of these fabrication methods, customizing of such tips is possible to a limited degree only. Hence, there is a need to complement pre-fabricated cantilevers with application-specific probes. Probes with colloidal tips, for instance, are typically obtained by gluing a sphere to the end of a cantilever.[9,10]

A similar approach is used for scanning-probe systems that cannot rely on optical readout approaches, such as the laser beam deflection method, or interferometry, to detect the probe position.[1,2] Self-sensing cantilevers based on piezoelectric[11] and piezoresistive[12,13] materials or tunnel magnetoresistance (TMR)[14] were developed, but these solutions do not provide integrated tips. Consequently, tips are commonly glued to such cantilevers by hand.[11,14,15]

In order to obtain hydrophobic tips, Kim and Maramatsu[16,17] introduced two-photon polymerization (TPP) as a tool to write AFM tips. They reported tip sizes below 100 nm and observed reduced adhesion forces of such polymeric tips. Jung *et al.*[18] added a tip to the end of an optical fiber by TPP and further decreased the tip radius to 15 nm in a subsequent step by O_2-plasma ashing. Lee *et al.*[19] used mold inserts to attach hydrogel probes. So far, tips written with three-dimensional lithography always resembled their conventionally fabricated counterparts. The potential of using arbitrary shapes was not exploited for the benefit of AFM. Here, we use latest 3D direct laser writing technology based on two-photon polymerization and add tips with arbitrary size and shape to the end of AFM cantilevers. This approach offers a large variety of options to design tips in order to obtain optimal conditions for the imaging of surfaces by AFM. We experimentally demonstrate the viability of the approach by directly writing sharp tips ($R \approx 25$ nm) in one lithography step. We further show exceptionally tall tips ($h > 100\,\mu$m), which are optimal for the imaging of surfaces with high aspect ratio features, or within deep trenches. Finally, we demonstrate that rebar structures can be written onto a cantilever to tune its resonance spectrum, for applications such as multifrequency AFM.

For 3D two-photon polymerization, an ultraviolet light (UV) curable resist is exposed to a tightly focused infrared (IR) femto-second light source. Two-photon absorption triggers a polymerization reaction. We utilized a commercial 3D-printer (Photonic Professional GT, Nanoscribe GmbH) to form AFM tips on cantilevers. The schematic setup, as well as an electron micrograph of a resulting structure, is shown

[a]G. Göring and P.-I. Dietrich contributed equally to this work.
[b]Electronic mail: hendrik.hoelscher@kit.edu

in Fig. 1(a). For the writing process, one or several cantilevers are fixed to a common substrate, such as a glass slide. After that, the substrate with all cantilevers is drop-cast in a resist (IP-Dip, Nanoscribe GmbH) that also serves as the immersion-medium for the objective (63×, NA = 1.4). A 3D-model of a tip is designed according to the needs of the application. It is sliced into layers parallel to the focal plane of the objective of the lithography tool. By scanning a writing focus along hatching lines within one layer, the resist is locally polymerized and thus hardened. The process starts at the cantilever (i.e., at the widest part of the tip), and for subsequent layers, the distance of the objective to the cantilever is increased. The writing speed for most of the structures was chosen as 20 mm/s, hatching and slicing distances were set to 100 nm. In order to obtain a sharp tip apex, the top part of the tip, typically the last 5 μm, was written with 50 nm hatching and slicing distance, and a writing speed of 1 mm/s.

The design and fabrication of tailored tips is especially useful for samples which cannot be imaged with a conventional tip, and many designs can be envisioned. Figures 1(b)–1(g) summarize various structures that were fabricated by direct laser writing. In general, any 3D-object within the writing field of the objective can be written in a coarse high-speed mode, and thereafter equipped with a tip. We applied this procedure to thin tips with high aspect-ratio, tips as long as 100 μm, round tips for adhesion measurement, and completely arbitrary shaped tips such as the Matterhorn (Figs. 1(b)–1(e)). We also prepared protruding tips (Fig. 1(f)) which are visible from the top, ensuring a clear view of the sample surface during scanning, making it easier to move the AFM-tip to the actual region of interest. Furthermore, the combination of AFM-imaging with optical spectroscopy is straightforward with such geometries.

It is also possible to convert the tips into carbon by employing a pyrolysis process.[20,21] Pyrolysis entails heating the patterned polymer structures up to 900 °C in an inert environment. Figure 1(g) shows a tip after carbonization. As is evident from this image, the resulting tip is much smaller in size owing to pyrolysis shrinkage.[20] Therefore, carbonization of these tips through pyrolysis opens a completely new field by allowing for the tips to be smaller in size than the lithography limit, electrically and thermally conductive, harder, biocompatible, and easy to functionalize.[21–23]

The advantage of tailored tips can be nicely demonstrated by the fabrication of long tips with high aspect ratio. Figure 2 compares two measurements of the *cuticula* of a rose petal. Such wax structures are present in many plants, and due to their interaction with light, optical investigation methods fail in many cases to characterize the morphology of plant surfaces such as rose petals. Figure 2 shows AFM images of a rose petal replica obtained by casting. From Fig. 2(a), it is obvious that a standard cantilever with a typical tip length of 10–15 μm is not suitable to image the rose petal structures correctly, because the nipple structures in the *cuticula* are much higher than the height of a conventional tip. During scanning, the tip cannot penetrate into cavities between the nipple-shaped protrusions, and the cantilever itself touches the sample leading to an inverted imaging process. The AFM cantilever is scanned by the nipples and the cantilever shape is observable in the topography image in Fig. 2(a). With two-photon polymerization, however, it is straightforward to write a sufficiently high aspect ratio tip on a tipless cantilever (or to overwrite an existing tip with a sufficiently high tip). Thus, it is possible to measure comparably high features or very deep structures with these optimized tips. Figure 2(b) shows the AFM image obtained with a tip

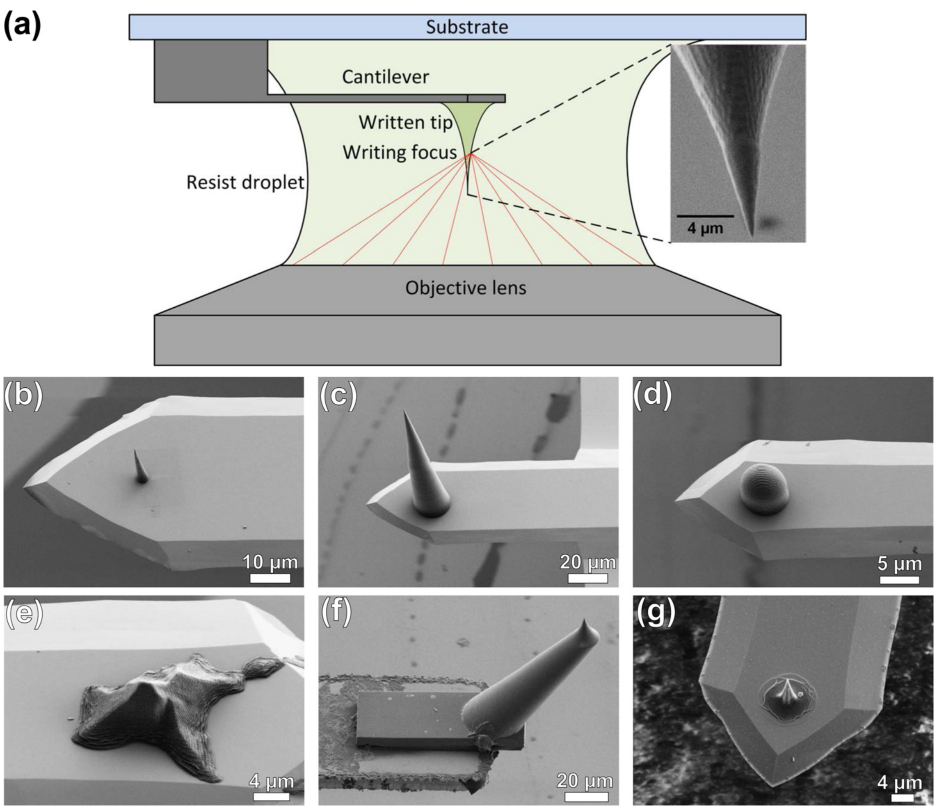

FIG. 1. (a) Schematic drawing of the writing process on the cantilever using two-photon polymerization. The inset in shows a SEM image of the tip apex. To obtain a sharp and defined tip apex, it was written with optimized (but slower) parameters. Therefore, the surface of the tip apex is smoother than the rest of the structure. A large variety of tips can be fabricated in this way. (b) High (20 μm) and thin (5 μm at the base) tip. (c) Extremely long tip with a height of 100 μm. (d) Spherical tip with diameter of 10 μm. (e) Tip in the shape of the famous Swiss mountain "Matterhorn." (f) Protruding tip that is visible from the top during scanning. (g) Shrunk conical tip after carbonization through pyrolysis.

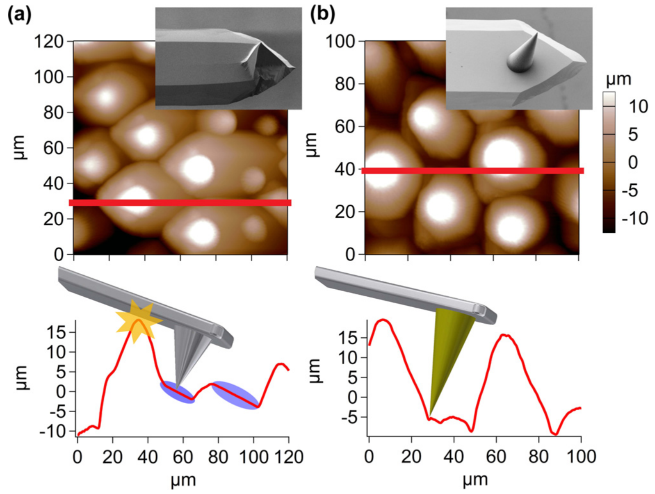

FIG. 2. (a) Image of a rose petal recorded with a conventional AFM tip. The SEM image in the inset shows the tip used (NSG10, NT-MDT). The height of the tip is in the typical range of 10–15 μm but not sufficient to image the comparably deep cavities between the nipples of the rose petal (blue marks). (b) Imaging of the same structure with a tailored tip with a height of 30 μm. The tip is shown in the inset. Due to the optimized geometry the rose petal is scanned correctly. Now all cavities can be penetrated and the nipples can be imaged in all detail.

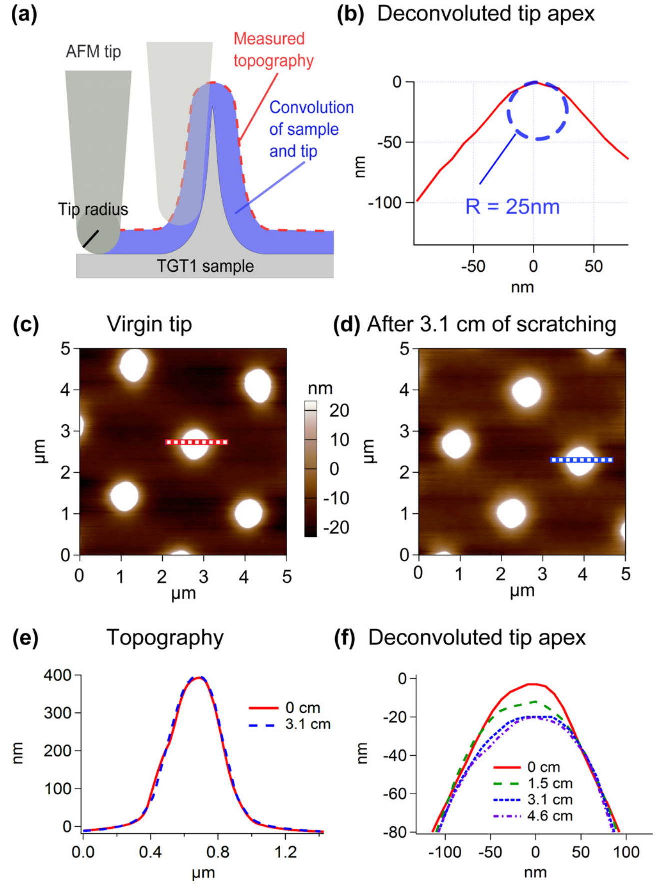

FIG. 3. (a) Schematic of the convolution of tip and sample. (b) Deconvoluted tip apex with a tip radius of 25 nm. (c) Initially obtained image of the grating. (d) Image recorded after 3.1 cm of contact mode scratching. (e) Overlay of the cross sections marked in the topography images (c) and (d). (f) Comparison of the tip forms calculated by deconvolution. Although we measured with a comparably high loading force in contact mode, the sharpness of the tip after several centimeters is still sufficient for imaging.

twice as high than a conventional one. All features of the rose petal surface can now be resolved down to the bottom of the crevices.

Tips written by 3D direct laser writing consist of a polymer (the developed resist) with a Young's modulus of 2.34 GPa.[24] Although the stiffness is sufficient for imaging, an immediately arising question is the long term stability of the polymer. We therefore analyzed the long-term stability of a tip by scanning a hard test grid for several hours (TGT1 test grid, NT-MDT). This sample is densely covered with sharp tips with a radius smaller than 10 nm. As the substrate radius is smaller than the radius of our polymeric tip, it allows us to determine the radius of our self-made tip by deconvolution (Deconvo2 software, NT-MDT). Figure 3(a) shows the basic principle of tip-sample convolution.[10,25] As expected, the radius can be as small as the curvature of the voxel (<25 nm). Hence, this technique also allows to survey voxel size and shape as written by two-photon polymerization.

To measure the abrasion of the tailored tips, we continuously scanned the TGT1 grating in contact mode, with a frequency of 0.1 Hz, and with a high loading force of (66 $\pm$ 10%) nN. Each scan consisted of 512 lines per trace and retrace, and a scan range of 5 μm, resulting into an effective lateral scratch distance of 5.12 mm per image. While for large features of a sample the contribution of the tip radius is negligible, the convolution of tip and sample increases when the features are in the range of the tip radius. If the features of the sample are even smaller, the tip is imaged by the sharp spikes on the TGT1 grid. To demonstrate the long-term stability of the tips, we compare the initial with the 6th image obtained after 3.1 cm of scratching in Figs. 3(c) and 3(d). Two cross sections of spikes on the sample taken from these two images demonstrate that the blunting of the tip had negligible influence on the obtained topography map. In Fig. 3(f), the deconvoluted curvatures of the tip are shown as a function of the scanning distance. The tip radius increased from 52 nm to 75 nm. Still, after 4.6 cm of scratching (or 9 images), the tip radius remains sufficient for imaging. Consequently, tip wear is within an acceptable range, despite the rough imaging conditions with regard to loading force.

Adding tips to cantilevers is only one application of 3D laser writing. Any arbitrary structure can be written at any position along the length of the AFM beam. This feature is, for example, useful to tune the resonance spectra of cantilevers, for multifrequency AFM, where higher eigenmodes of the cantilever are excited in addition to the first one.[26–28] Figure 4 shows how the resonance frequencies of different cantilevers are tuned to obtain optimized frequency spectra. The unstructured cantilevers are surveyed and subsequently structurally reinforced with a light framework. Depending on the form and size of the framework, the dynamical properties of the cantilever are modified. Modes can be selectively suppressed, employing the absorptive nature of the polymer,[29] by adding polymer structures which interact differently with different modes. For example, a properly placed gap in a rebar structure can facilitate the excitation of a specific higher order mode, which does not significantly deform the polymer and hence exhibits significantly lower losses than, e.g., the ground mode. Due to the additional mass of the polymeric rebar structure all resonance peaks shift to lower

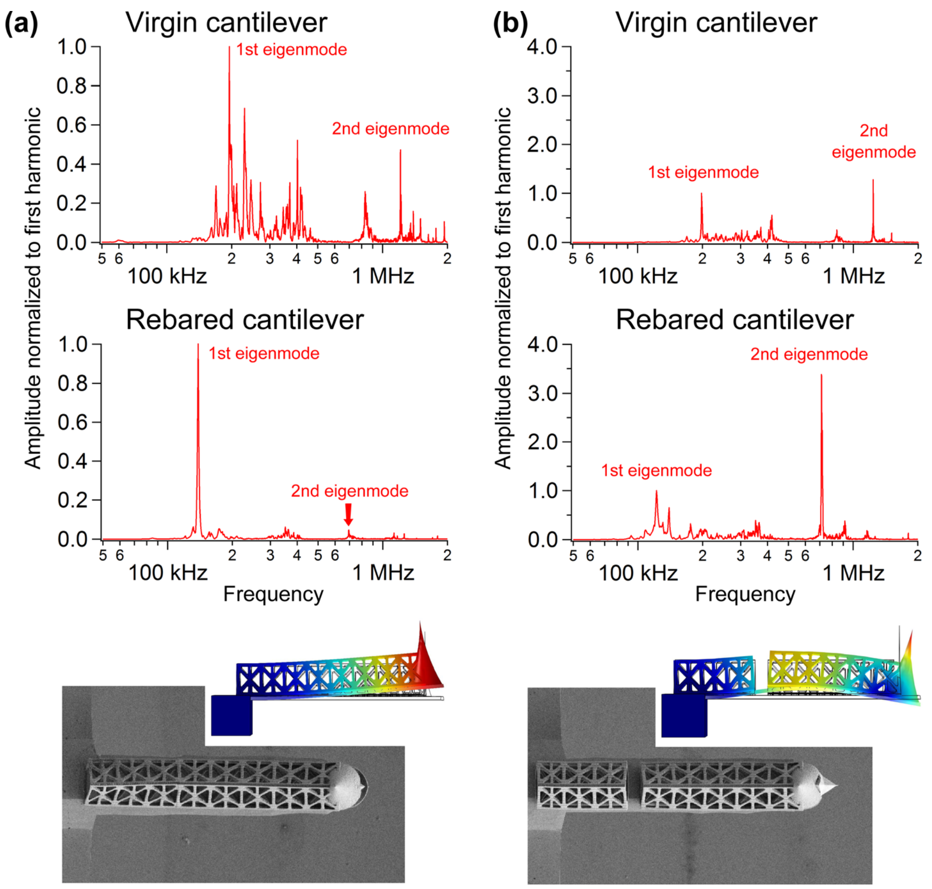

FIG. 4. Adding rebar structures to cantilevers allows to tune their resonance spectrum. The upper graphs shows the spectra of two virgin cantilevers while the middle ones were recorded after the addition of rebar structures. The SEM images of the written structures at the bottom are combined with insets of animations of the corresponding modes. The color code corresponds to the displacement. (a) The resonance spectrum of a conventional AFM cantilever has several peaks and is shown on the top. The signal height is normalized to the first eigenmode at $f_0 = 198$ kHz. Adding a continuous rebar structure to the rectangular cantilever suppresses higher eigenmodes as well as noise. The first eigenmode of the cantilever is strongly enhanced. (b) Leaving a gap in the rebar structure stimulates the second eigenmode compared to the unstructured cantilever. Now the second eigenmode is greatly enhanced while the first eigenmode and noise are suppressed.

frequencies. In Fig. 4(a), we added a continuous rebar structure to the cantilever which is stiffened in this way. Now, only the first eigenmode stands out in the spectrum and unwanted resonances and noise are suppressed. The second eigenmode, however, can be enhanced by weakening the rebar structure near the node of the second cantilever eigenmode. Figure 4(b) shows such a rebar structure, and the spectrum demonstrates that the amplitude of the second eigenmode is greatly enhanced. Finite element simulations of the deformation of the modified cantilevers agree with experimental observations.

To conclude, AFM tips with arbitrary shapes can be added to existing AFM cantilevers by 3D direct laser writing. These tips are mechanically stable and optimize AFM probes for their desired task. Tuning frequencies of a cantilever with rebar structures is also possible which is helpful for dynamic modes such as multi-frequency AFM. Future work will include the fabrication of complete AFM probes together with their cantilever which will be especially useful for the combination of AFM with other microscopy techniques.

It is a pleasure to thank Stefan Hengsbach and Richard Thelen for inspiring discussions and their kind help. The rose petal sample shown in Fig. 2 was provided by Raphael Schmager, Ruben Hönig, and Guillaume Gomard from the Light Technical Institute (LTI). G.G. and H.H. acknowledge support from the DFG grant (HO-2237-4-2). P.-I.D., M.B., and C.K. acknowledge support by the European Research Council (ERC Starting Grant "EnTeraPIC," No. 280145), by the Alfried Krupp von Bohlen und Halbach Foundation, and the BMBF joint project PHOIBOS. S.S. and J.G.K. acknowledge funding from the ERC (Senior Grant No. 290586-NMCEL). This work was partly carried out with the support of the Karlsruhe Nano Micro Facility (KNMF, www.kit.edu/knmf), a Helmholtz Research Infrastructure at Karlsruhe Institute of Technology (KIT, www.kit.edu).

[1]E. Meyer, H. J. Hug, and R. Bennewitz, *Scanning Probe Microscopy–The Lab on a Tip* (Springer-Verlag, Heidelberg, 2004).
[2]P. Eaton and P. West, *Atomic Force Microscopy* (Oxford University Press, Oxford, 2010).
[3]U. D. Schwarz, H. Haefke, P. Reimann, and H. J. Güntherodt, J. Microsc. **173**, 183 (1994).
[4]G. Dai, H. Wolff, F. Pohlenz, H.-U. Danzebrink, and G. Wilkening, Appl. Phys. Lett. **88**, 171908 (2006).
[5]O. Sahin, S. Magonov, C. Su, C. F. Quate, and O. Solgaard, Nat. Nanotechnol. **2**, 507 (2007).
[6]S. D. Solares and H. Hölscher, J. Vac. Sci. Technol., B **28**, C4E1 (2010).
[7]S. D. Solares and H. Hölscher, Nanotechnology **21**, 075702 (2010).
[8]O. Wolter, T. Bayer, and J. Greschner, J. Vac. Sci. Technol., B **9**, 1353 (1991).
[9]L. H. Mak, M. Knoll, D. Weiner, A. Gorschlüter, A. Schirmeisen, and H. Fuchs, Rev. Sci. Instrum. **77**, 046104 (2006).
[10]J.-E. Schmutz, M. M. Schäfer, and H. Hölscher, Rev. Sci. Instrum. **79**, 026103 (2008).
[11]F. J. Giessibl, Appl. Phys. Lett. **73**, 3956 (1998).
[12]M. Tortonese, R. C. Barrett, and C. F. Quate, Appl. Phys. Lett. **62**, 834 (1993).
[13]S. Hafizovic, D. Barrettino, T. Volden, J. Sedivy, K. U. Kirstein, O. Brand, and A. Hierlemann, Proc. Natl. Acad. Sci. U. S. A. **101**, 17011 (2004).
[14]A. Tavassolizadeh, T. Meier, K. Rott, G. Reiss, E. Quandt, H. Hölscher, and D. Meyners, Appl. Phys. Lett. **102**, 153104 (2013).
[15]J. Falter, M. Stiefermann, G. Langewisch, P. Schurig, H. Hölscher, H. Fuchs, and A. Schirmeisen, Beilstein J. Nanotechnol. **5**, 507 (2014).
[16]J. M. Kim and H. Maramatsu, Nano Lett. **5**, 309 (2005).
[17]W.-S. Kim, K.-M. Park, J. J. Park, S.-M. Chang, I.-H. Kim, H. Muramatsu, and J. M. Kim, Curr. Appl. Phys. **7**, 528 (2007).

[18]B. J. Jung, H. J. Kong, Y.-H. Cho, C. H. Park, M. K. Kim, B. G. Jeon, D.-Y. Yang, and K.-S. Lee, Curr. Appl. Phys. **13**, 2064 (2013).
[19]J. S. Lee, J. Song, S. O. Kim, S. Kim, W. Lee, J. A. Jackman, D. Kim, N.-J. Cho, and J. Lee, Nat. Commun. **7**, 11566 (2016).
[20]S. Sharma, A. Sharma, Y.-K. Cho, and M. Madou, ACS Appl. Mater. Interfaces **4**, 34 (2012).
[21]J. Bauer, A. Schroer, R. Schwaiger, and O. Kraft, Nat. Mater. **15**, 438–443 (2016).
[22]O. Schueller, S. T. Brittain, C. Marzolin, and G. M. Whitesides, Chem. Mater. **9**, 1399 (1997).
[23]S. Sharma and M. Madou, Bioinspired, Biomimetic Nanobiomater. **1**, 252 (2012).
[24]J. Bauer, A. Schroer, R. Schwaiger, I. Tesari, C. Lange, L. Valdevit, and O. Kraft, Extreme Mech. Lett. **3**, 105 (2015).
[25]B. Bhushan and K. J. Kwak, Appl. Phys. Lett. **91**, 163113 (2007).
[26]N. F. Martinez, S. Patil, J. R. Lozano, and R. Garcia, Appl. Phys. Lett. **89**, 153115 (2006).
[27]R. Proksch, Appl. Phys. Lett. **89**, 113121 (2006).
[28]D. Ebeling and S. D. Solares, Nanotechnology **24**, 135702 (2013).
[29]J. Hossenlopp, L. Jiang, R. Cernosek, and F. Josse, J. Polym. Sci.: Polym. **42**, 2373 (2004).